



Article

Gadolinium Chloride Rescues Niemann–Pick Type C Liver Damage

Andrés D. Klein ^{1,*}, Juan Esteban Oyarzún ², Cristian Cortez ³ and Silvana Zanlungo ^{2,*}

¹ Centro de Genética y Genómica, Facultad de Medicina, Clínica Alemana Universidad del Desarrollo, Santiago 7590943, Chile

² Departamento de Gastroenterología, Facultad de Medicina, Pontificia Universidad Católica de Chile, Santiago 8331150, Chile; jeoyarzu@uc.cl

³ Center for Genomic and Bioinformatic, Faculty of Sciences, Universidad Mayor, Santiago 8580745, Chile; Cristian.cortezplaza@umayor.cl

* Correspondence: andresklein@udd.cl (A.D.K.); szanlungo@uc.cl or silvana.zanlungo@gmail.com (S.Z.); Tel.: +56-2-2578-5778 (A.D.K.); +56-2-2354-383 (S.Z.)

Received: 29 September 2018; Accepted: 2 November 2018; Published: 14 November 2018



Abstract: Niemann–Pick type C (NPC) disease is a rare neurovisceral cholesterol storage disorder that arises from loss of function mutations in the *NPC1* or *NPC2* genes. Soon after birth, some patients present with an aggressive hepatosplenomegaly and cholestatic signs. Histopathologically, the liver presents with large numbers of foam cells; however, their role in disease pathogenesis has not been explored in depth. Here, we studied the consequences of gadolinium chloride ($GdCl_3$) treatment, a well-known Kupffer/foam cell inhibitor, at late stages of NPC liver disease and compared it with *NPC1* genetic rescue in hepatocytes in vivo. $GdCl_3$ treatment successfully blocked the endocytic capacity of hepatic Kupffer/foam measured by India ink endocytosis, decreased the levels CD68—A marker of Kupffer cells in the liver—and normalized the transaminase levels in serum of NPC mice to a similar extent to those obtained by genetic *Npc1* rescue of liver cells. Gadolinium salts are widely used as magnetic resonance imaging (MRI) contrasts. This study opens the possibility of targeting foam cells with gadolinium or by other means for improving NPC liver disease. **Synopsis:** Gadolinium chloride can effectively rescue some parameters of liver dysfunction in NPC mice and its potential use in patients should be carefully evaluated.

Keywords: Niemann–Pick type C disease; gadolinium chloride; liver disease; cholesterol; therapeutic option

1. Introduction

Niemann–Pick type C (NPC) is a fatal pediatric neurovisceral cholesterol storage disorder caused by loss of function mutations in the *NPC1* or *NPC2* genes. Both genes encode lysosomal proteins involved in the efflux of free cholesterol from lysosomes [1]. As consequence of these mutations, free cholesterol and other lipids accumulate in NPC lysosomes, generating cellular damage. Although several mechanisms have been postulated to explain the pathogenesis of the disease, the signaling pathways that are specifically affected have not yet been fully elucidated.

The estimated frequency of this disease is 1:100,000 live births [2] and affects many organs including the brain, liver, spleen, and lungs [3]. Some patients develop early liver dysfunction, which is particularly relevant for the infantile forms of the disease. Indeed, a recent study [4] reported the clinical features of 10 NPC patients who developed the disease in the newborn period between 1993 and 2015 and concluded that neonatal presentation is a rare form of NPC with exclusive visceral involvement in the newborn period and poor prognosis leading to premature death due to pulmonary

complications and liver failure. About 50% of classic NPC patients suffer from neonatal cholestasis, jaundice, and enlarged liver and/or spleen [5,6]. Of these patients, approximately 10% die from liver failure before they reach 6 months of age [7].

We and other researchers have reported progressive inflammation, oxidative stress, apoptosis, and fibrosis in the liver of a murine model of the disease (*Npc1*^{-/-} mice) [8–10]. From a histopathological perspective, NPC livers show large amounts of CD68-positive foam cells; however, their role in disease pathogenesis has been poorly characterized. It has been proposed that accumulation of Kupffer cells loaded with lipids would lead to the consequent secretion of inflammatory cytokines, such as TNF α and profibrotic TGF-beta [9,11]. This response, in other diseases with hepatic lesions, leads to the recruitment and activation of hepatic stellate cells (HSC), triggering fibrosis and apoptosis. In this scenario, Kupffer cells would have an essential role in NPC liver pathogenesis. To test this hypothesis, we treated NPC mice with gadolinium chloride (GdCl₃), a well-known Kupffer/foam cell inhibitor [12].

GdCl₃ has been widely used to examine the relevance of Kupffer cells in the pathogenesis of several liver diseases. In fact, it has been used in different models, including drug-induced damage, arsenic toxicity, diet-induced hepatic steatosis, and insulin resistance and ischemia–reperfusion [13–16]. In these and other studies, it was reported that GdCl₃ prevents or diminishes liver damage. More recently, Yang et al. demonstrated that GdCl₃ attenuated liver inflammation and fibrosis in two liver injury models (methionine-choline deficient and high fat (MCDHF) and carbon tetrachloride (CCl₄)) [17]. On the other hand, Kupffer cell inhibition can induce detrimental effects. It has been observed that treatment with GdCl₃ decreases hepatic regeneration after partial liver transplantation [18]. Similarly, the work of Zhu et al. shows that Kupffer cell depletion by gadolinium chloride aggravates liver injury after brain death in rats [19].

Besides inhibiting the endocytosis of Kupffer cells, GdCl₃ depletes the M1 subpopulation of macrophages. This subset of cells corresponds to proinflammatory macrophages activated by LPS and Th1 proinflammatory cytokines, such as IFN γ , TNF α , and IL-1 β . GdCl₃ would not affect the M2 subset, macrophages that participate in resolution of inflammation, and comprises various forms of nonclassically activated macrophages originating from exposure to different stimuli, such as the Th2 cytokines IL-4, IL-13, IL-10, and TGF β [20].

Gadolinium salts are widely used in clinics as MRI contrasts [21]. These salts have been used for studying the in vivo function of Kupffer cells, since circulating monocytes and other macrophages are less vulnerable to them [22]. In the present study, we evaluated the effects of GdCl₃ on NPC liver disease and we compared them with a genetic rescue of NPC1 protein in hepatocytes in vivo, which was previously shown to be sufficient to decrease liver pathology [23].

2. Results

To study the kinetics of hepatic macrophage infiltration, we analyzed the levels of CD68 staining by immunofluorescence. No foam cells were found in wild-type (WT) mice, whereas increased staining was observed in NPC (*Npc1*^{-/-}) tissues. Moreover, the levels of the staining positively correlated with the age of the *Npc1*^{-/-} mice (Figure 1A), suggesting that foam cells might play a role in liver pathogenesis. To further characterize the extent of foam cell infiltration at late stages of disease progression, we performed a three-dimensional reconstruction (z-stacks) of representative liver sections from 9-week-old animals. *Npc1*^{-/-} livers showed many round-shape CD68 foam cells compared to wild-type (WT) tissues (Figure 1B).

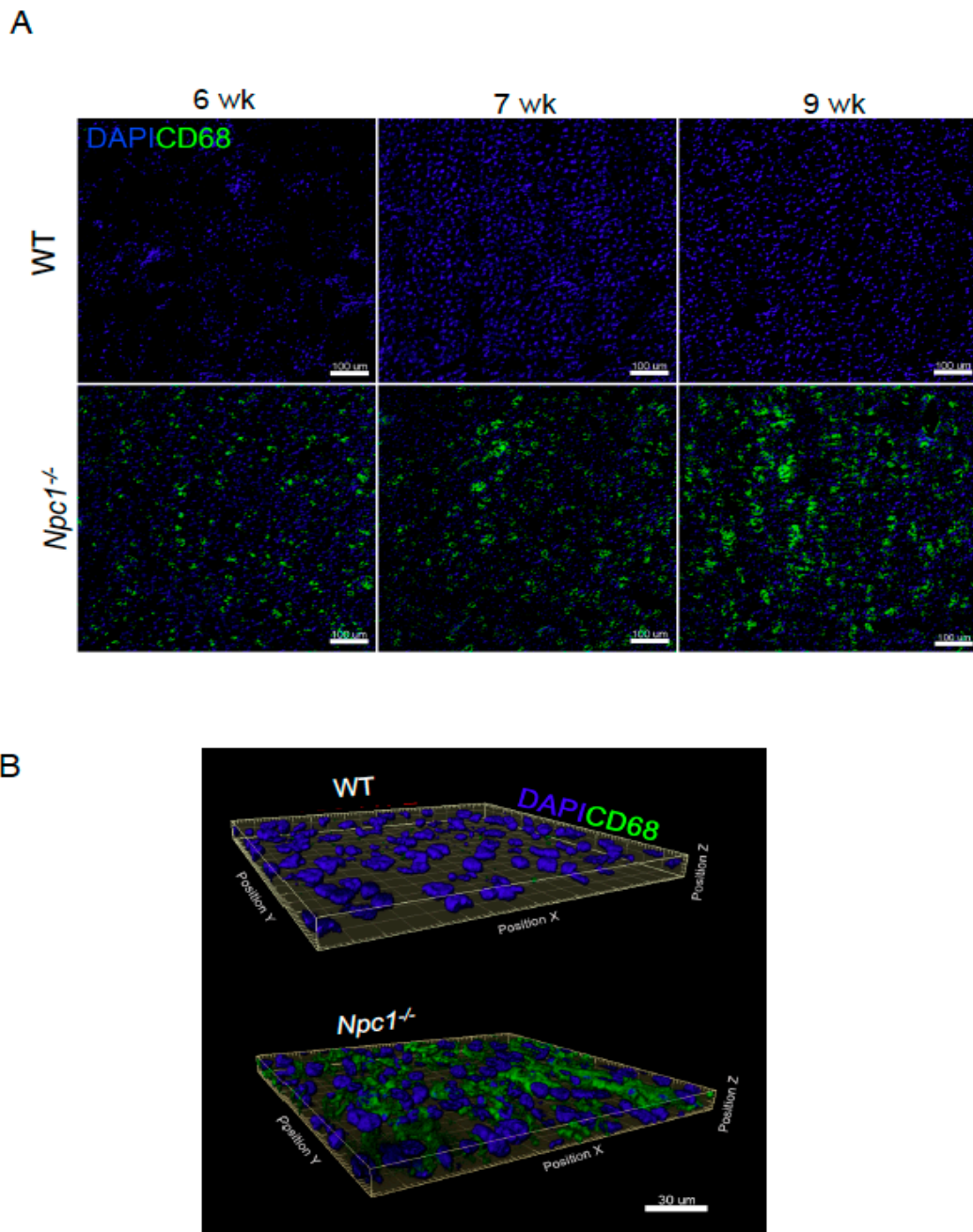


Figure 1. Progressive increase of hepatic CD68 positive cells in Niemann–Pick type C (NPC) mice. (A) CD68 staining of livers from 6-, 7-, and 9-week-old (wk) wild-type (WT) and *Npc1*^{−/−} mice. Scale bars are 100 μm. (B) Three-dimensional reconstructions of liver sections from 9-week-old WT and *Npc1*^{−/−} mice.

Next, we analyzed the extent of reversibility of foam cell numbers after rescuing hepatic NPC1 by genetic means. For this purpose, we used a previously developed genetic tool to express a tagged-NPC1 protein in hepatocytes *in vivo* based on the tet system [23,24]. Upon doxycycline (DOX) administration to *Npc1*^{−/−} transgenic mice for ROSA26-rtTA-M2 and TRE-*Npc1*-YFP (abbreviated R; N), NPC1-YFP was expressed. Hepatocyte correction was sufficient to rescue NPC liver damage [23]. We then continued characterizing this effect in terms of the number of foam cells. We allowed the disease to progress for 49 days, when mice already show liver disease, and we fed them with DOX for 1 week (Figure 2A). Tissues were stained with hematoxylin and eosin at postnatal day 56 (Figure 2B). As previously shown for the BALB/c background, wild-type animals did not show the presence foam

cells. Livers from nonrescued *Npc1*^{-/-} mice showed a large number of foam cells/area unit, which was significantly reduced upon DOX treatments (Figure 2C). Therefore, we hypothesized that inhibition of foam cells may have a positive impact on NPC liver disease.

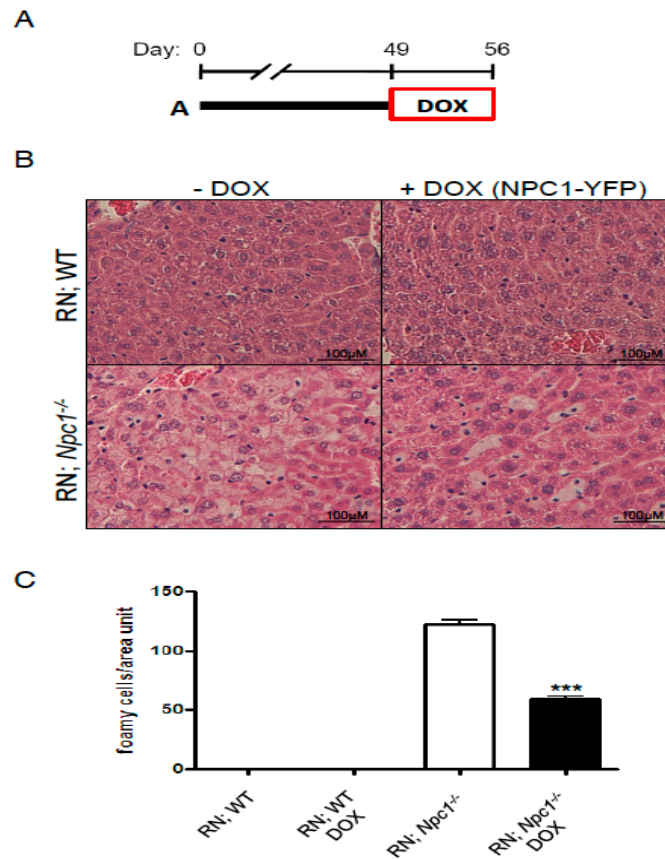


Figure 2. Foam-cell-associated NPC liver pathology is corrected by genetic NPC1 rescue. **(A)** Timeline of the duration and age of doxycycline (DOX) treatment in mice. **(B)** Expression of the NPC1-YFP transgene, driven by Rosa-rtTA in ROSA26-rtTA-M2 and TRE-Npc1-YFP (R; N), WT, or *Npc1*^{-/-} mice, was induced with DOX on day 49. After 1 week of treatment, animals were sacrificed and livers were processed for histological analysis by Hematoxylin and eosin staining. Scale bars are 100 µm. **(C)** Quantification of the number of foam cells in each condition. *** $p < 0.0001$.

If activation of foam cell activity plays a detrimental role in NPC liver disease, their inhibition should exert beneficial effects. To test the technical feasibility of inhibiting hepatic Kupffer/foam cell endocytosis, we treated animals with GdCl₃ from postnatal day (P)49–P56 followed by one India ink injection (Figure 3A). We decided to treat *Npc1*^{-/-} animals starting from P49 because at this stage, they already showed extensive liver damage, including increased alanine transaminase (ALT) and inflammation [10,23]. We chose the therapeutic dose of 10 mg/kg of GdCl₃ because it had been successfully used before in models presenting hepatic buildup of lipids and in other animal models with liver extensive damage [16,25,26]. The saline-treated animals showed high levels of India ink deposits in the liver with a distribution pattern consistent with Kupffer cell morphology in WT animals and foam cells in *Npc1*^{-/-} mice. These deposits were difficult to find in animals pretreated with GdCl₃ (Figure 3B), indicating that gadolinium effectively blocks the endocytic properties of these cells under WT conditions and also in the context of NPC disease.

To characterize the effects of blocking NPC foam cell endocytosis and their cholesterol buildup, we stained liver sections with CD68 and filipin. GdCl₃-treated livers have a decreased number of CD68 cells and CD68 cells positive for filipin. This effect can be visualized in the merged images (Figure 3C) and it was also quantified (Figure 3D,E). GdCl₃ not only blocks endocytosis but also depletes the M1 subpopulation of macrophages in WT animals [22]. To test the effects of GdCl₃ in an NPC context, we used CD68 staining as a general marker of Kupffer/foam cells. Interestingly, GdCl₃ treatment from P49 to P56 reduced the area covered by CD68 cells (Figure 3E). Finally, to determine the effect of GdCl₃ treatment on liver disease, we measured the levels of the ALT enzyme in plasma (Figure 4A). Importantly, we found that GdCl₃ significantly reduced ALT levels in NPC mice to levels very similar to those produced by genetic rescue of NPC1 (Figure 4B).

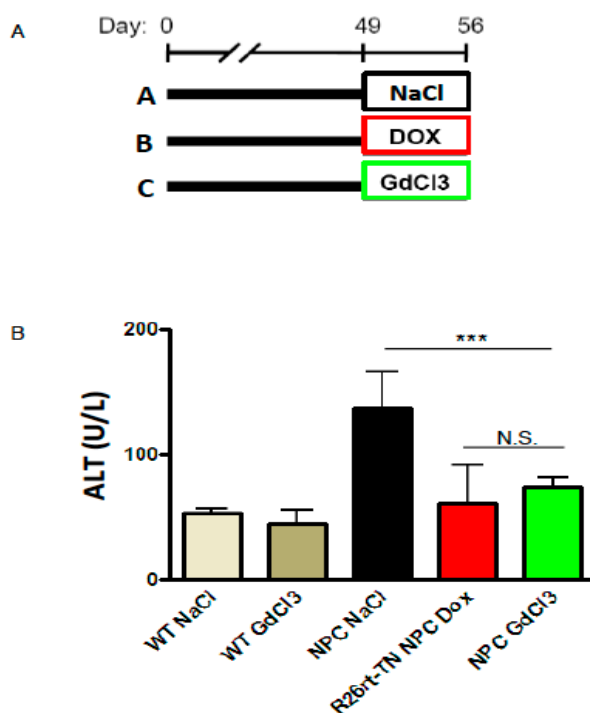


Figure 4. Foam-cell-associated NPC liver pathology is improved by GdCl₃ treatment. (A) Timeline of the duration and age of different treatments in mice. (B) Alanine transaminase (ALT) levels in the different groups. Data are presented as means \pm SD. ($n = 3\text{--}5$ animals/group, two-way ANOVA, and Tukey's multiple comparison post-test). *** $p < 0.0001$.

Together these results show that GdCl₃ can effectively rescue Niemann–Pick type C liver ALT increase in mice.

3. Discussion

Although neuronal damage is the major cause of death in NPC, most patients have considerable liver damage. In fact, several studies indicate that between 45% and 65% of NPC patients develop liver disorders, including cholestasis, prolonged jaundice, and hepatomegaly [5,6]. The engagement of immune pathways in NPC pathogenesis has shown disparate results [27–31]. In this study, we demonstrated that GdCl₃ decreased the endocytic capacity of Kupffer/foam cells and normalized transaminase levels in serum of NPC mice to a similar extent to those obtained by NPC1 genetic rescue of liver cells.

Gadolinium treatment has shown beneficial effects in several models of liver diseases, including alcoholic liver disease [32], nonalcoholic fatty liver [13], liver failure following acetaminophen intoxication [33], ischemia–reperfusion injury [14], amiodarone [16], and others. Amiodarone-induced liver damage is particularly interesting for our work since it induces a Niemann–Pick-type-C-like

phenotype in cells [34]. In animal models, 10 mg/kg of $GdCl_3$ has been shown to be safe. However, 50 mg/kg induces kidney toxicity [35]. In humans, there is still debate about the $GdCl_3$ safety range. To date, the main reported adverse symptom is nephrogenic systemic fibrosis in patients with renal disease already present. These patients do not receive $GdCl_3$ but other Gd-based contrasts. However, it should be kept in mind that $GdCl_3$ can be accumulated in the human body, inducing kidney toxicity and potentially the dysfunction of other organs by unknown mechanisms [36]. Toxicity depends on the molecular stability of the drug, which varies together with the pharmacokinetic properties of each compound and also depends on the individual characteristics of the subject [37]. In children, the rate of Gd-induced acute adverse nephropathy is lower than in adults [38]. However, recent findings indicate that Gd can accumulate in other tissues, including the brain, in patients with normal renal function. These data added renewed concerns regarding Gd long-term toxicity [39].

The mechanisms by which $GdCl_3$ exerts its beneficial effects on livers of NPC mice are not entirely clear. However, they are not mediated by NPC1 (since $GdCl_3$ can rescue a NPC1 deficient mice) but rather by modulating signaling pathways triggered by uncontrolled lipid uptake by macrophages. It is very likely that macrophages from genetically rescued livers secrete lower levels of inflammatory chemokines and cytokines because they have been uptaking lower amounts of lipids. A potential downstream effector of NPC macrophages that could be blocked by $GdCl_3$ is $TNF\alpha$, which has been previously shown to play a role in hepatic NPC pathophysiology [9]. Therefore, $GdCl_3$ effects could be directly related to the inactivation of Kupffer cells in response to the accumulation of cholesterol and/or to a reduction in the secretion of cytokines such as $TNF\alpha$. Indeed, a large number of studies show that Gd^{3+} is a selective Kupffer cell inhibitor that lowers Kupffer cell number and phagocytic activity [40–43]. Moreover, Vincent et al. (2010) showed that antibodies against $TNF\alpha$ decreased some parameters of liver damage in NPC mice [44]. Another possibility is that gadolinium could correct calcium homeostasis or sphingosine accumulation, which are disease hallmarks [45,46]. The increase in lysosomal sphingosine levels would increase the release of calcium from NPC lysosomes, emptying their stores [47]. Release of lysosomal calcium is required for lysosome trafficking and fusion with other cellular compartments, such as autophagosomes and the plasma membrane [48]. Increasing the expression or activity of the Mucopolipin 1 or TRPML1 lysosomal ion channel is sufficient to correct the trafficking defects and reduce lysosome storage and cholesterol accumulation in NPC cells [49]. Interestingly, Gd^{3+} is a lanthanide that exhibits properties similar to that of calcium in biological systems, presumably due to its comparable ionic radius [50], and is detected in lysosomes of hepatocytes and Kupffer cells [51]. Considering these antecedents, gadolinium could potentially activate TRPML1. According to this idea, we found that gadolinium slightly decreased filipin staining in CD68 positive cells in the treated mice. These results suggest that the mechanism by which $GdCl_3$ exerts its beneficial effects is mediated through the inhibition of foam cell endocytosis rather than other cell types, such as hepatocytes. However, we cannot discard direct effects of $GdCl_3$ on hepatocytes. To our knowledge, there are few reports showing protective effects of $GdCl_3$ treatments in isolated hepatocytes. It was shown that Gd^{3+} can reduce the levels of cytochrome P450 in hepatocytes [52], which in turn can reduce oxidative damage. Oxidative damage is an important feature in NPC; therefore, Gd^{3+} can contribute to the beneficial effects observed in vivo.

In addition, the effects of $GdCl_3$ could be related to its activity as an inducer of the macrophage M1 subpopulation depletion [22]. Interestingly, we have previously shown that treatment with clodronate, which mainly depletes M2 macrophages [53], enhanced NPC liver damage [23]. Further studies are required to determine the mechanisms by which gadolinium improves liver disease in NPC mice.

Recent studies show that it is possible to improve liver disease in NPC by trying combined therapies that include cyclodextrin to decrease the accumulation of cholesterol. Alam et al. (2016) obtained outstanding results, both in viscera and CNS, treating an NPC mouse model with the pan-HDAC inhibitor (HDACi) vorinostat, 2-hydroxypropyl- β -cyclodextrin (HPBCD), and polyethylene glycol (PEG) [54]. Ebner et al. (2018) tried a combination of HP β CD, miglustat, and allopregnanolone, obtaining a decrease in hepatic lipids and an amelioration of mouse NPC liver

disease symptoms [55]. In this sense, gadolinium can be visualized as an alternative for a combination therapy along with other drugs such as cyclodextrin, capable of lowering the cholesterol burden, specifically directed to improve liver function in NPC disease.

In summary, our work shows that gadolinium inhibits Kupffer cell activity and normalizes ALT levels in serum of NPC mice. Our research opens the possibility of targeting foam cells with gadolinium or by other means for improving NPC liver disease.

4. Materials and Methods

4.1. Mice

BALB/c *Npc1*^{+/-} mice, originally purchased from Jackson Laboratory (Bar Harbor, ME), were bred to generate our own colony at Pontificia Universidad Católica de Chile (PUC). Genotypes (*Npc1*^{+/+}; WT and *Npc1*^{-/-}; NPC) were identified as described previously [56]. In addition, we used *Npc1*^{-/-} mice in the FVB background, which develop a disease indistinguishable from the animals in the BALB/c background [23,24]. Transgenic *ROSA26-rtTA-M2; TRE-Npc1-YFP, Npc1*^{-/-} mice for liver rescue were in the FVB genetic background. The breeding strategy to generate *Npc1*^{-/-} transgenic mice for *ROSA26-rtTA-M2* and *TRE-Npc1-YFP* (R;N) and genotyping protocols have been previously reported [24]. *Npc1*^{-/-} mice in the FVB background were used for GdCl₃ treatments to compare the results with the genetic rescue experiments. The experiments performed with animals in the FVB background were done at Stanford University School of Medicine and those performed in the BALB/c background were executed at PUC. Protocols were performed according to accepted criteria for the humane care of experimental animals and were approved by the institutional review board of both institutions (Stanford Administrative Panel on Laboratory Animal Care (APLAC) protocol #10412 and Scientific Ethics Committee for the Care of Animals and the Environment, Pontificia Universidad Católica de Chile #160321008 (exCEBA 14-038), approved on 6 November 2014).

4.2. Treatments

All mice had free access to water and chow diet (<0.02% cholesterol; Prolab RMH 3000, PMI Feeds Inc., St. Louis, MO, USA) until they were used for the studies. Doxycycline (Sigma, Kawasaki City, Japan) was administered in the drinking water at 2 mg/mL in 5% sucrose, every 3 days, from P49–P56. GdCl₃ (Sigma, Kawasaki City, Japan) was injected at 10 mg/Kg i.v. (dissolved in NaCl 0.9%) on days 49 and 53, and tissues and the liver enzymes were processed on day 56. India ink injections were administered i.v. 30 min before sacrificing the animals as previously described [57].

4.3. Liver and Blood Sampling

Mice were anesthetized by intraperitoneal injection of ketamine (80–100 mg/kg) and xylazine (5–10 mg/kg). After sacrificing the animals, blood was extracted from the inferior vena cava. Blood was centrifuged at 4000 rpm for 20 min at 4 °C to recover the plasma, which was subsequently stored at –20 °C.

4.4. Liver ALT

ALT plasma level analysis was performed in-house at the Stanford University Veterinary Service.

4.5. Histology

For the BALB/c *Npc1*^{+/+} and *Npc1*^{-/-} mice, fresh tissues were frozen in liquid nitrogen. They were sectioned with a cryostat in 8-µm slices and then mounted on slides. They were fixed for 30 min in 4% paraformaldehyde. The cryosections were washed three times with 0.05% PBS-tween. Then, they were permeabilized with 0.1% Triton, blocked at room temperature for 1 h in 4% BSA, and incubated with the mouse anti-CD68 antibody (1:1000; Serotec, Kidlington, UK). CD68 was detected using an anti-rat donkey antibody conjugated with Cy3 (1:500; Jackson Immuno Research Laboratories,

West Grove, PA, USA). Confocal images of immunostained tissue were acquired with a Leica TCS SP8 laser-scanning microscope (Leica, Wetzlar, Germany). The series of images obtained from confocal z-stacks were processed and analyzed using Leica LAS AF (Leica, 2012, Wetzlar, Germany). In addition, 3D reconstructions of z-stack image data obtained from wild-type or *Npc1*^{-/-} slices acquired in confocal microscopy were processed and analyzed using the Imaris software (Bitplane, Zürich, Switzerland).

For the animals in the FVB background, procedures were performed as previously described [23,58]. Briefly, free-floating liver sections were blocked for 1 h with 2% BSA/0.2% Triton X-100 in PBS and incubated overnight with a rat anti-CD68 antibody (1:1000; Serotec, Kidlington, UK). CD68 was detected using a Cy3-conjugated donkey anti-rat antibody (1:200; Jackson Immuno Research Laboratories, West Grove, PA, USA). Filipin was obtained from Sigma. The percent area of tissue positive for CD68 immunofluorescence was measured using the ImageJ 1.50i software (NIH, Bethesda, MD, USA) as previously described [24]. Hematoxylin and eosin staining was performed by the pathological anatomy facility at Stanford University. To detect India ink deposits, livers were removed 30 min postinjection, fixed in 4% paraformaldehyde overnight, and sectioned with a Vibratome into 40- μ m slices. Tissues were mounted on a cover slide and observed directly with a Zeiss Axioplan2 microscope equipped with an AxioCam HRc CCD camera. Confocal images were obtained with a Leica TCS SP2 laser-scanning microscope. Quantification of the number of foam cells in the genetically rescued mice and the filipin-positive CD68 cells were performed manually. Quantification of CD68 fluorescence was performed as previously described [24]. Briefly, CD68 staining was converted to binary data by manual thresholding using ImageJ [59], so that the space occupied by the resulting black image approximated the area of fluorescence. The percentage area occupied by black pixels was then measured and the SEM reported.

4.6. Statistical Analyses

Statistical analyses were performed using GraphPad Prism 6 (Graphpad Software Inc., San Diego, CA, USA). ANOVA followed by Tukey's multiple comparison test were used for statistical comparisons between the groups. Data in graphs are shown as mean \pm SEM.

Author Contributions: A.D.K. and S.Z. participated in the design and analysis of all the experiments and in the writing of the manuscript. A.D.K. developed most of the experiments. J.E.O. and C.C. participated in some experiments and their analysis.

Funding: This research was funded by Fondecyt (grant #1180337 to A.D.K. and #1150186 to S.Z.), CONICYT-PCHA/Doctorado-Nacional/ grant #2014-62968 to J.E.O. and by the European Union's Horizon 2020 research and innovation programme (RISE) under the Marie Skłodowska-Curie grant agreement #.734825.

Acknowledgments: We thank Matthew P. Scott from Stanford University for facilitating his lab resources to perform many of the experiments. We want to acknowledge Manuel Lopez for technical support.

Conflicts of Interest: The authors declare no conflicts of interest.

References

1. Kwon, H.J.; Abi-Mosleh, L.; Wang, M.L.; Deisenhofer, J.; Goldstein, J.L.; Brown, M.S.; Infante, R.E. Structure of N-Terminal Domain of NPC1 Reveals Distinct Subdomains for Binding and Transfer of Cholesterol. *Cell* **2009**, *137*, 1213–1224. [[CrossRef](#)] [[PubMed](#)]
2. Geberhiwot, T.; Moro, A.; Dardis, A.; Ramaswami, U.; Sirrs, S.; Marfa, M.P.; Vanier, M.T.; Walterfang, M.; Bolton, S.; Dawson, C.; et al. Consensus clinical management guidelines for Niemann–Pick disease type C. *Orphanet J. Rare Dis.* **2018**, *13*, 50. [[CrossRef](#)] [[PubMed](#)]
3. Klein, A.D.; Alvarez, A.; Zanlungo, S. The unique case of the Niemann–Pick type C cholesterol storage disorder. *Pediatr. Endocrinol. Rev.* **2014**, *12*, 166–175. [[PubMed](#)]
4. Gumus, E.; Haliloglu, G.; Karhan, A.N.; Demir, H.; Gurakan, F.; Topcu, M.; Yuce, A. Niemann–Pick disease type C in the newborn period: A single-center experience. *Eur. J. Pediatr.* **2017**, *176*, 1669–1676. [[CrossRef](#)] [[PubMed](#)]

5. Yerushalmi, B.; Sokol, R.J.; Narkewicz, M.R.; Smith, D.; Ashmead, J.W.; Wenger, D.A. Niemann–Pick disease type C in neonatal cholestasis at a North American Center. *J. Pediatr. Gastroenterol. Nutr.* **2002**, *35*, 44–50. [[CrossRef](#)] [[PubMed](#)]
6. Yang, R.; Tan, D.; Wang, Y.; Ye, J.; Han, L.; Qiu, W.; Gu, X.; Zhang, H. [Three Chinese children with Niemann–Pick disease type C with neonatal cholestasis as initial presentation]. *Zhonghua er ke za zhi (Chin. J. Pediatr.)* **2015**, *53*, 57–61.
7. Kelly, D.A.; Portmann, B.; Mowat, A.P.; Sherlock, S.; Lake, B.D. Niemann–Pick disease type C: Diagnosis and outcome in children, with particular reference to liver disease. *J. Pediatr.* **1993**, *123*, 242–247. [[CrossRef](#)]
8. Rimkunas, V.M.; Graham, M.J.; Crooke, R.M.; Liscum, L. In vivo antisense oligonucleotide reduction of NPC1 expression as a novel mouse model for Niemann Pick Type C- associated liver disease. *Hepatology* **2008**, *47*, 1504–1512. [[CrossRef](#)] [[PubMed](#)]
9. Rimkunas, V.M.; Graham, M.J.; Crooke, R.M.; Liscum, L. TNF- α plays a role in hepatocyte apoptosis in Niemann–Pick type C liver disease. *J. Lipid Res.* **2009**, *50*, 327–333. [[CrossRef](#)] [[PubMed](#)]
10. Vázquez, M.C.; del Pozo, T.; Robledo, F.A.; Carrasco, G.; Pavez, L.; Olivares, F.; González, M.; Zanlungo, S. Alteration of gene expression profile in Niemann–Pick type C mice correlates with tissue damage and oxidative stress. *PLoS ONE* **2011**, *6*, e28777. [[CrossRef](#)] [[PubMed](#)]
11. Vanier, M.T. Niemann–Pick diseases. *Handb. Clin. Neurol.* **2013**, *113*, 1717–1721. [[PubMed](#)]
12. Husztko, E.; Lázár, G.; Párducz, A. Electron microscopic study of Kupffer-cell phagocytosis blockade induced by gadolinium chloride. *Br. J. Exp. Pathol.* **1980**, *61*, 624–630. [[PubMed](#)]
13. Huang, W.; Metlakunta, A.; Dedousis, N.; Zhang, P.; Sipula, I.; Dube, J.J.; Scott, D.K.; O’Doherty, R.M. Depletion of liver Kupffer cells prevents the development of diet-induced hepatic steatosis and insulin resistance. *Diabetes* **2010**, *59*, 347–357. [[CrossRef](#)] [[PubMed](#)]
14. Wang, B.; Zhang, Q.; Zhu, B.; Cui, Z.; Zhou, J. Protective Effect of Gadolinium Chloride on Early Warm Ischemia/Reperfusion Injury in Rat Bile Duct during Liver Transplantation. *PLoS ONE* **2013**, *8*, e52743. [[CrossRef](#)] [[PubMed](#)]
15. Adeyemi, O.S.; Meyakno, E.; Akanji, M.A. Inhibition of Kupffer cell functions modulates arsenic intoxication in Wistar rats. *Gen. Physiol. Biophys.* **2017**, *2*, 219–227. [[CrossRef](#)] [[PubMed](#)]
16. Takai, S.; Oda, S.; Tsuneyama, K.; Fukami, T.; Nakajima, M.; Yokoi, T. Establishment of a mouse model for amiodarone-induced liver injury and analyses of its hepatotoxic mechanism. *J. Appl. Toxicol.* **2016**, *36*, 35–47. [[CrossRef](#)] [[PubMed](#)]
17. Yang, L.; Yang, L.; Dong, C.; Li, L. The class D scavenger receptor CD68 contributes to mouse chronic liver injury. *Immunol. Res.* **2018**, *3*, 414–424. [[CrossRef](#)] [[PubMed](#)]
18. Luo, H.Y.; Ma, S.F.; Qu, J.F.; Tian, D.H. Effects of Kupffer cell inactivation on graft survival and liver regeneration after partial liver transplantation in rats. *Hepatobiliary Pancreat. Dis. Int.* **2015**, *1*, 56–62. [[CrossRef](#)]
19. Zhu, R.; Guo, W.; Fang, H.; Cao, S.; Yan, B.; Chen, S.; Zhang, K.; Zhang, S. Kupffer cell depletion by gadolinium chloride aggravates liver injury after brain death in rats. *Mol. Med. Rep.* **2018**, *17*, 6357–6362. [[CrossRef](#)] [[PubMed](#)]
20. Raggi, F.; Pelassa, S.; Pierobon, D.; Penco, F.; Gattorno, M.; Novelli, F.; Eva, A.; Varesio, L.; Giovarelli, M.; Bosco, M.C. Regulation of human Macrophage M1-M2 Polarization Balance by hypoxia and the Triggering receptor expressed on Myeloid cells-1. *Front. Immunol.* **2017**, *8*, 1097. [[CrossRef](#)] [[PubMed](#)]
21. Gale, E.M.; Caravan, P.; Rao, A.G.; McDonald, R.J.; Winfeld, M.; Fleck, R.J.; Gee, M.S. Gadolinium-based contrast agents in pediatric magnetic resonance imaging. *Pediatr. Radiol.* **2017**, *47*, 507–521. [[CrossRef](#)] [[PubMed](#)]
22. Hardonk, M.J.; Dijkhuis, F.W.; Hulstaert, C.E.; Koudstaal, J. Heterogeneity of rat liver and spleen macrophages in gadolinium chloride-induced elimination and repopulation. *J. Leukoc. Biol.* **1992**, *52*, 296–302. [[CrossRef](#)] [[PubMed](#)]
23. Lopez, M.E.; Klein, A.D.; Hong, J.; Dimbil, U.J.; Scott, M.P. Neuronal and epithelial cell rescue resolves chronic systemic inflammation in the lipid storage disorder Niemann–Pick C. *Hum. Mol. Genet.* **2012**, *21*, 2946–2960. [[CrossRef](#)] [[PubMed](#)]
24. Lopez, M.E.; Klein, A.D.; Dimbil, U.J.; Scott, M.P. Anatomically defined neuron-based rescue of neurodegenerative Niemann–Pick type C disorder. *J. Neurosci.* **2011**, *31*, 4367–4378. [[CrossRef](#)] [[PubMed](#)]
25. Mosher, B.; Dean, R.; Harkema, J.; Remick, D.; Palma, J.; Crockett, E. Inhibition of Kupffer cells reduced CXC chemokine production and liver injury. *J. Surg. Res.* **2001**, *99*, 201–210. [[CrossRef](#)] [[PubMed](#)]

26. Chen, L.; Ye, H.; Zhao, X.; Miao, Q.; Li, Y.; Hu, R. Selective depletion of hepatic kupffer cells significantly alleviated hepatosteatosis and intrahepatic inflammation induced by high fat diet. *Hepatogastroenterology*. **2012**, *59*, 1208–1212. [[CrossRef](#)] [[PubMed](#)]
27. Lopez, M.E.; Klein, A.D.; Scott, M.P. Complement is dispensable for neurodegeneration in Niemann–Pick disease type C. *J. Neuroinflammation* **2012**, *9*, 216. [[CrossRef](#)] [[PubMed](#)]
28. Cougnoux, A.; Cluzeau, C.; Mitra, S.; Li, R.; Williams, I.; Burkert, K.; Xu, X.; Wassif, C.A.; Zheng, W.; Porter, F.D. Necroptosis in Niemann–Pick disease, type C1: A potential therapeutic target. *Cell Death Dis.* **2016**, *7*, e2147. [[CrossRef](#)] [[PubMed](#)]
29. Smith, D.; Wallom, K.L.; Williams, I.M.; Jeyakumar, M.; Platt, F.M. Beneficial effects of anti-inflammatory therapy in a mouse model of Niemann–Pick disease type C1. *Neurobiol. Dis.* **2009**, *36*, 242–251. [[CrossRef](#)] [[PubMed](#)]
30. Calderón, J.F.; Klein, A.D. Controversies on the potential therapeutic use of rapamycin for treating a lysosomal cholesterol storage disease. *Mol. Genet. Metab. Reports* **2018**, *15*, 135–136. [[CrossRef](#)] [[PubMed](#)]
31. Platt, N.; Speak, A.O.; Colaco, A.; Gray, J.; Smith, D.A.; Williams, I.M.; Wallom, K.L.; Platt, F.M. Immune dysfunction in Niemann–Pick disease type C. *J. Neurochem.* **2016**, *136*, 74–80. [[CrossRef](#)] [[PubMed](#)]
32. Koop, D.R.; Klopfenstein, B.; Iimuro, Y.; Thurman, R.G. Gadolinium chloride blocks alcohol-dependent liver toxicity in rats treated chronically with intragastric alcohol despite the induction of CYP2E1. *Mol. Pharmacol.* **1997**, *51*, 944–950. [[CrossRef](#)] [[PubMed](#)]
33. Michael, S.L.; Pumford, N.R.; Mayeux, P.R.; Niesman, M.R.; Hinson, J.A. Pretreatment of mice with macrophage inactivators decreases acetaminophen hepatotoxicity and the formation of reactive oxygen and nitrogen species. *Hepatology* **1999**, *30*, 186–195. [[CrossRef](#)] [[PubMed](#)]
34. Piccoli, E.; Nadai, M.; Caretta, C.M.; Bergonzini, V.; Del Vecchio, C.; Ha, H.R.; Bigler, L.; Dal Zoppo, D.; Faggini, E.; Pettenazzo, A.; et al. Amiodarone impairs trafficking through late endosomes inducing a Niemann–Pick C-like phenotype. *Biochem. Pharmacol.* **2011**, *82*, 1234–1249. [[CrossRef](#)] [[PubMed](#)]
35. Liao, P.; Wei, L.; Zhang, X.; Li, X.; Wu, H.; Wu, Y.; Ni, J.; Pei, F. Metabolic profiling of serum from gadolinium chloride-treated rats by 1H NMR spectroscopy. *Anal. Biochem.* **2007**, *364*, 112–121. [[CrossRef](#)] [[PubMed](#)]
36. Ramalho, J.; Ramalho, M.; Jay, M.; Burke, L.M.; Semelka, R.C. Gadolinium toxicity and treatment. *Magn. Reson. Imaging* **2016**, *34*, 1394–1398. [[CrossRef](#)] [[PubMed](#)]
37. Pasquini, L.; Napolitano, A.; Visconti, E.; Longo, D.; Romano, A.; Tomà, P.; Espagnet, M.C. R. Gadolinium-Based Contrast Agent-Related Toxicities. *CNS Drugs* **2018**, *32*, 229–240. [[CrossRef](#)] [[PubMed](#)]
38. Soares, B.P.; Lequin, M.H.; Huisman, T.A.G.M. Safety of Contrast Material Use in Children. *Magn. Reson. Imaging Clin. N. Am.* **2017**, *25*, 779–785. [[CrossRef](#)] [[PubMed](#)]
39. Ramalho, J.; Ramalho, M. Gadolinium Deposition and Chronic Toxicity. *Magn. Reson. Imaging Clin. N. Am.* **2017**, *25*, 765–778. [[CrossRef](#)] [[PubMed](#)]
40. O'Neill, P.J.; Ayala, A.; Wang, P.; Ba, Z.F.; Morrison, M.H.; Schultze, A.E.; Reich, S.S.; Chaudry, I.H. Role of Kupffer cells in interleukin-6 release following trauma-hemorrhage and resuscitation. *Shock* **1994**, *1*, 43–47. [[CrossRef](#)] [[PubMed](#)]
41. Iimuro, Y.; Yamamoto, M.; Kohno, H.; Itakura, J.; Fujii, H.; Matsumoto, Y. Blockade of liver macrophages by gadolinium chloride reduces lethality in endotoxemic rats—Analysis of mechanisms of lethality in endotoxemia. *J. Leukoc. Biol.* **1994**, *55*, 723–728. [[CrossRef](#)] [[PubMed](#)]
42. Vollmar, B.; Rüttinger, D.; Wanner, G.A.; Leiderer, R.; Menger, M.D. Modulation of Kupffer cell activity by gadolinium chloride in endotoxemic rats. *Shock* **1996**, *6*, 434–441. [[CrossRef](#)] [[PubMed](#)]
43. Yu, S.; Nakafusa, Y.; Flye, M.W. In vitro analysis of gadolinium chloride abrogation of the systemic tolerance induced by portal venous administration of ultraviolet B-irradiated donor cells. *In Transplantation*; **1997**, *64*, 1684–1688. [[CrossRef](#)]
44. Vincent, M.; Sayre, N.L.; Graham, M.J.; Crooke, R.M.; Shealy, D.J.; Liscum, L. Evaluation of an anti-tumor necrosis factor therapeutic in a mouse model of Niemann–Pick C liver disease. *PLoS ONE* **2010**, *5*, e12941. [[CrossRef](#)] [[PubMed](#)]
45. Pelled, D.; Trajkovic-Bodenec, S.; Lloyd-Evans, E.; Sidransky, E.; Schiffmann, R.; Futerman, A.H. Enhanced calcium release in the acute neuronopathic form of Gaucher disease. *Neurobiol. Dis.* **2005**, *18*, 83–88. [[CrossRef](#)] [[PubMed](#)]
46. Platt, F.M. Emptying the stores: Lysosomal diseases and therapeutic strategies. *Nat. Rev. Drug Discov.* **2018**, *17*, 133–150. [[CrossRef](#)] [[PubMed](#)]

47. Höglinger, D.; Haberkant, P.; Aguilera-Romero, A.; Riezman, H.; Porter, F.D.; Platt, F.M.; Galione, A.; Schultz, C. Intracellular sphingosine releases calcium from lysosomes. *Elife* **2015**, *4*, e10616. [[CrossRef](#)] [[PubMed](#)]
48. Medina, D.L.; Di Paola, S.; Peluso, I.; Armani, A.; De Stefani, D.; Venditti, R.; Montefusco, S.; Scotto-Rosato, A.; Prezioso, C.; Forrester, A.; et al. Lysosomal calcium signalling regulates autophagy through calcineurin and TFEB. *Nat. Cell Biol.* **2015**, *17*, 288–299. [[CrossRef](#)] [[PubMed](#)]
49. Shen, D.; Wang, X.; Li, X.; Zhang, X.; Yao, Z.; Dibble, S.; Dong, X.P.; Yu, T.; Lieberman, A.P.; Showalter, H.D.; et al. Lipid storage disorders block lysosomal trafficking by inhibiting a TRP channel and lysosomal calcium release. *Nat. Commun.* **2012**, *3*, 731. [[CrossRef](#)] [[PubMed](#)]
50. Lansman, J.B. Blockade of current through single calcium channels by trivalent lanthanide cations. Effect of ionic radius on the rates of ion entry and exit. *J. Gen. Physiol.* **1990**, *95*, 679–696. [[CrossRef](#)] [[PubMed](#)]
51. Ahlem, A.; Ali, E.H.; Leila, T. Lysosomes of the liver and the duodenal enterocytes, a site of handling of two rare earths. Ultrastructural and microanalytical study. *Biol. Trace Elem. Res.* **2008**, *124*, 40–51. [[CrossRef](#)] [[PubMed](#)]
52. Hirasawa, F.; Kawagoe, M.; Wang, J.S.; Arany, S.; Zhou, X.P.; Kumagai, A.; Koizumi, Y.; Koyota, S.; Sugiyama, T. Gadolinium chloride suppresses styrene-induced cytochrome P450s expression in rat liver. *Biomed. Res* **2007**, *28*, 323–330. [[CrossRef](#)] [[PubMed](#)]
53. Laskin, D.L. Macrophages and inflammatory mediators in chemical toxicity: A battle of forces. *Chem. Res. Toxicol.* **2009**, *22*, 1376–1385. [[CrossRef](#)] [[PubMed](#)]
54. Alam, M.S.; Getz, M.; Haldar, K. Chronic administration of an HDAC inhibitor treats both neurological and systemic Niemann–Pick type C disease in a mouse model. *Sci. Transl. Med.* **2016**, *8*, 326ra23. [[CrossRef](#)] [[PubMed](#)]
55. Ebner, L.; Gläser, A.; Bräuer, A.; Witt, M.; Wree, A.; Rolfs, A.; Frank, M.; Vollmar, B.; Kuhla, A. Evaluation of two liver treatment strategies in a mouse model of niemann–pick-disease type C1. *Int. J. Mol. Sci.* **2018**, *19*, 972. [[CrossRef](#)] [[PubMed](#)]
56. Amigo, L.; Mendoza, H.; Castro, J.; Quiones, V.; Miquel, J.F.; Zanlungo, S. Relevance of Niemann–Pick type C1 protein expression in controlling plasma cholesterol and biliary lipid secretion in mice. *Hepatology* **2002**, *36*, 819–828. [[CrossRef](#)] [[PubMed](#)]
57. Janzen, E.G.; Chen, J.Z.; Reinke, L.A.; Yamashiro, S. Inhibitory effect of phenyl N-terf-butyl nitron on Kupffer cell phagocytosis. *Redox Rep.* **1996**, *2*, 345–347. [[CrossRef](#)] [[PubMed](#)]
58. Klein, A.D.; Ferreira, N.-S.; Ben-Dor, S.; Duan, J.; Hardy, J.; Cox, T.M.; Merrill, A.H.; Futerman, A.H. Identification of Modifier Genes in a Mouse Model of Gaucher Disease. *Cell Rep.* **2016**, *16*, 613–618. [[CrossRef](#)] [[PubMed](#)]
59. Schneider, C.A.; Rasband, W.S.; Eliceiri, K.W. NIH Image to ImageJ: 25 years of image analysis. *Nat. Methods* **2012**, *9*, 671–675. [[CrossRef](#)] [[PubMed](#)]

